Mass Balance and its Connection to Surge Events on Lowell Glacier, Yukon, Canada

Simon A. Campbell

34982165

GEOB 408 – Snow and Ice Process

Research Project

April 3, 2019

1. Introduction

Surge-type glaciers are characterized by regular periodic alternations of fast and slow ice-flow, typically referred to as active and quiescent phases respectively (Meier & Post, 1969). Controls on the surging process are divided between two theoretical initiation mechanisms: threshold behavior of underlying sediments, and changes in subglacial meltwater drainage system (Sharp, 1988).

Surging in the Alaska-Yukon region has been described as a net increase in ice thickness taking place in the accumulation zone during the quiescent phase, followed by rapid advance of the terminus due to ice being transported into the accumulation zone during the active phase (Meier and Post, 1969; Kamb et al., 1985). Furthermore, studies in the Alaska-Yukon region and St. Elias Mountains have provided evidence for glacier mass balance as a control on the recurrence interval between active surge events (Abe et al., 2016; Bevington and Copland, 2014; Eisen et al., 2001), and similar findings have been recorded in the Karakoram Himalaya (Copland et al., 2011) and in the Norweigan high arctic (Dowdeswell et al., 1995).

However, the precise relationship between mass balance and cyclic surging events remains unclear and is different between regions. In this study, we expand on previous work on the Lowell Glacier, Yukon, Canada to better understand this relationship. Specifically, we quantify changes in equilibrium line altitude (ELA) over time as a proxy for annual mass balance. We then correlate these changes with the past three surge events of the Lowell glacier. This involves an assessment of how the ELA timeseries is responding to quiescent and active surge phases, as well as surge characteristics and proposed initiation mechanism theories. Based on regional observations presented in previously published work (Abe et al., 2016; Eisen et al., 2001), we expect to see a positive mass balance trend during quiescent periods due to ice buildup in the accumulation zone, followed by a negative mass balance during the active surge phase due to ice thinning from increases in surface area shown in (Bevington and Copland, 2014).

2. Study Area and Background

The highest concentration of surge type glaciers in North America is located in the Alaska-Yukon region, with the majority occurring in the St. Elias Mountains, Yukon (Clarke and Holdsworth, 2002). Extensive ice cover and highly variable displays of surging behaviour make the St. Elias Mountains an important region in glaciological research, as recent work has been motivated in part by the acceleration of observed changes taking place in the area. The vast ice cover in the area will have a considerable impact on sea level rise due to a warming climate. (Flowers et al., 2014).

The Lowell Glacier (Lat: 60.28768, Lon: -138. 073941) is a large valley glacier located near the eastern limit of the St Elias Mountains, south-west of Haines Junction, Yukon, Canada (Fig.1). It shares an accumulation area with the nearby Fisher, Dusty and Hubbard Glaciers, and flows east from the St. Elias Icefields (~1500 m a.s.l) to Lowell lake at ~480 m a.s.l (Bevington and Copland, 2014). Lowell Glacier is of particular interest to both local populations and researchers due of recent activity showing large reservoirs of supra-glacial meltwater generated in the high accumulation zone (AGU, 2019), as well as evidence of terminus advances during previous surges which caused the damming of the Alsek River and subsequent inundated of the present town site of Haines Junction (Clague and Rampton, 1982). Bevington and Copland (2014) characterized the past five surges of Lowell Glacier. The first recorded surge event took place on 1948 (A1), followed by 1968 (A2), 1983 (A3), 1997 (A4) and 2009 (A5). They provide details on how area, length, and ice-velocity respond to surge events, and provide insight to the possible surging initiation mechanisms and controls on recurrence intervals (Fig. 2). As stated previously, we will expand on these findings by looking at the correlation between annual mass balance and the past three surging events (A3-5).

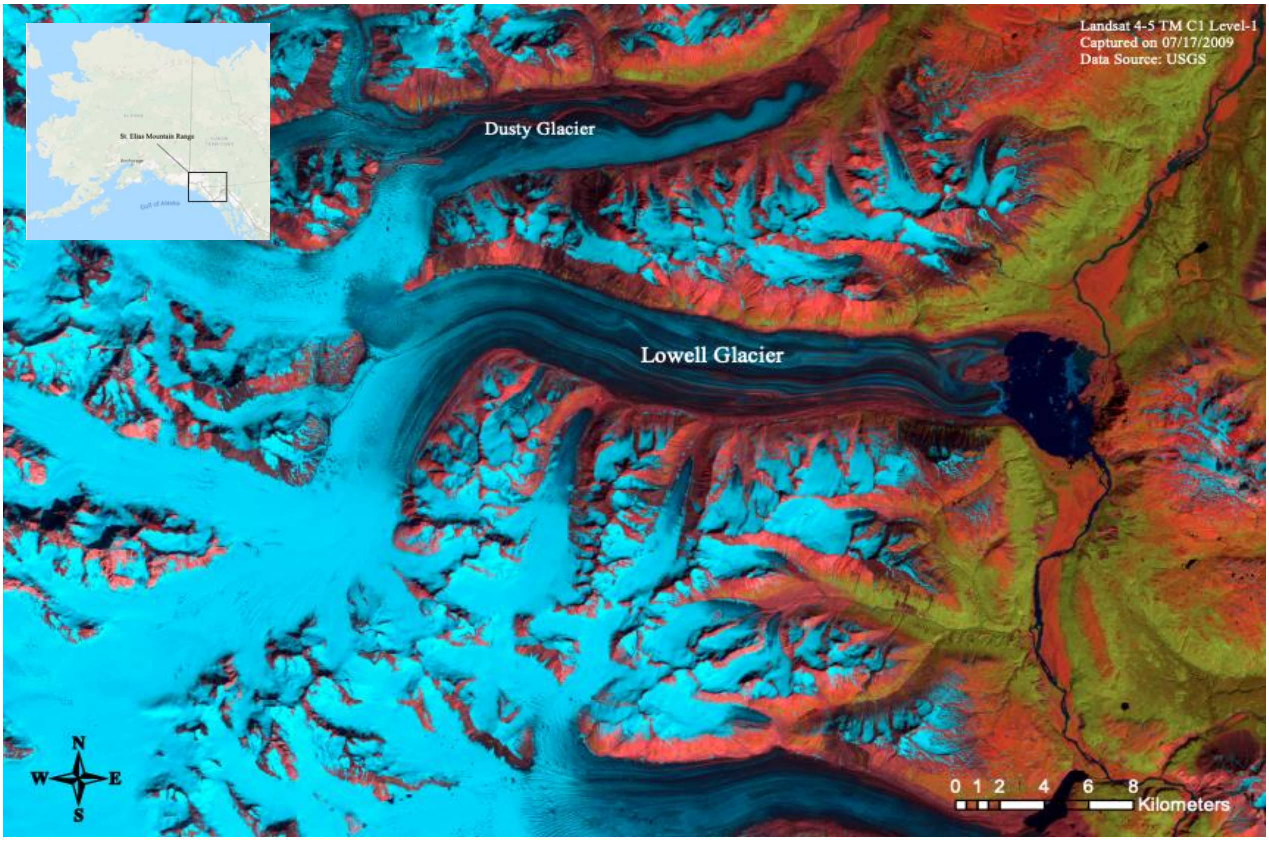

Fig. 1. Overview of the Lowell Glacier: LANDSAT 5 TM C1 Level 1 image, captured on July 17th, 2009. False colour band combination used to highlight the contrast between snow (light blue) and bare ice (dark blue) from surrounding terrain. Map created using ESRI ArcGIS 10.6.1. Data Source: United States Geological Survey, Global Visualization Viewer.

3. Data and Methods

3.1. Satellite Imagery

Table 1: Satellite imagery used in this study

Satellite	Spatial Resolution (meters)	Acquisition Date (yyyy-mm-dd)
Landsat-1 (L1) MSS	60	1973-09-13, 1975-09-22, 1977-09-27
Landsat-2 (L2) MSS	60	1976-08-01, 1978-08-28
Landsat-3 (L3) MSS	60	1980-08-26
Landsat-4 (L4) MSS/TM	60, 30	1983-08-28, 1984-08-21, 1985-08-24, 1986-09-03
Landsat-5 (L5) MSS/TM	60, 30	1988-09-09, 1989-08-27, 1990-08-23, 1992-08-26, 1993-09-14, 1994-08-18, 1995-09-06, 1996-09-06, 1998-08-13, 1999-07-31, 2003-08-11, 2004-08-13
Landsat-1 (L7) ETM+	30	2001-08-13, 2005-08-15, 2006-08-09, 2007-08-28 2008-08-30, 2009-08-03, 2010-09-14, 2011-07-22, 2016-08-20
Landsat-1 (L8) OLI/TIRS	30	2013-08-13, 2014-08-23, 2015-08-03, 2017-08-08, 2018-09-03

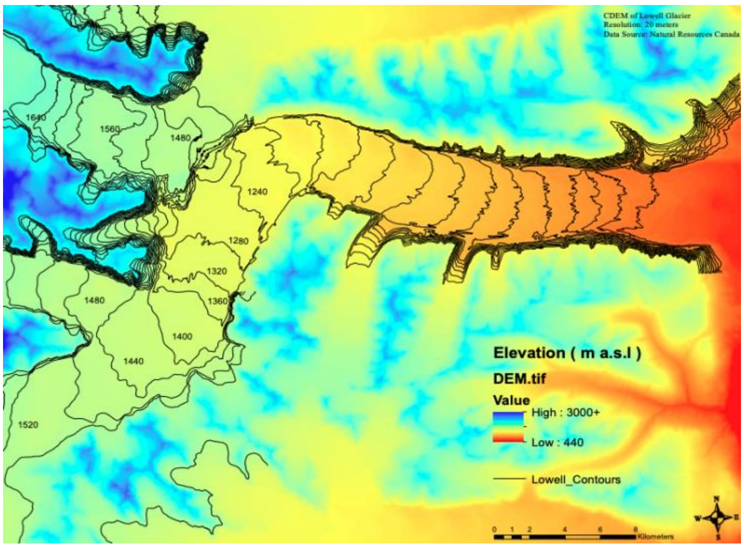

Fig. 2. Canadian Digital Elevation Model of Lowell Glacier with CanVec Contour Elevation overlay. Data source: Government of Canada Open Data Portal. Snowline elevations determined by visual approximation.

To track and quantify ELA over time, we used a collection of satellite images from 1973-2018. Due to the sparse availability of high-resolution images in the pre-satellite-mage era (<1972), ELA was monitored for only the past three surges of Lowell Glacier. For the satellite-image era (>1973), 36 LANDSAT images were used (Table 1). These images were retrieved from the United States Geological Survey Global Visualisation Viewer as georeferenced level-1 data (https://glovis.usgs.gov/), and processed using ESRI ArcGIS 10.6.1. A false colour band combination was used to provide contrast between bare ice, snow and water bodies, and only images with little to no (< 20%) cloud cover were chosen to allow for clear viewing of the glacier surface. Data was used from Landsat 4-8 satellites, with spatial resolutions varying from 30 - 60 meters. These images were used to track the location the snowline (firn-line) at the end of the balance year (late August – early September). Images captured during this time period were used whenever possible, however this was not applicable for some years (e.g. 1999 and 2011) due to unavailability of data. All images in table 1 refer to those used in approximating ELA over time.

3.2. Elevation Data

To determine the snowline altitude, 40 meter contour polygons from the Government of Canada Open Data Portal CanVec series were used as a reference along the glacier (fig. 2). A high resolution (20 m) Canadian Digital Elevation Model (CDEM) was used in conjunction with contour data for more accurate approximations of snowline altitude. Elevation data was retrieved from the GC Geospatial Data Extraction Tool (https://maps.canada.ca/czs/index-en.html).

3.3. Reconstructing (Relative) Mass Balance from ELA

Remotely-sensed imagery provides a useful and important tool for identifying the ELA in remote areas where field observations are lacking (Østrem, 1975). Since ELA is equivalent to the snowline at the end of the balance year (Braithwaite and Raper, 2009; Mernild et al., 2003; Østrem, 1975), remotely sensed images and elevation data were able to give a reliable approximation of the maximum ELA for the Lowell Glacier from 1973-2018. This altitude corresponds to where the net annual mass balance (defined as the net glacier mass balance from the onset of the accumulation season to the end of the following ablation season) on the glacier is zero (accumulation = ablation), where an increase/decrease in ELA between balance years corresponds to a net negative/positive mass balance respectively (Mernild et al., 2013; Hock et al., 2007). Therefore, a time series of maximum ELA each year will highlights relative variations in mass balance – that is, an increasing/decreasing ELA will be indicative of a net negative/positive mass balance relative to the previous year (Fig. 3).

3.4 Error and Uncertainty

Although the ELA - mass balance relationship is well established (Hock et al., 2007; Mernild et al., 2013; Østrem, 1975; Pelto, 2011), it should be noted that the methods presented here are purely qualitative and do not reflect precise mass balance measurements; we will be using the term ‘relative mass balance’ as a generalization of net annual mass balance year to year. Therefore, our analysis will be based on the assumption that net positive / negative changes in mass balance are reflected in the movement of the ELA respective to Lowell Glacier. Mass balance calculation techniques such as field measurements and accumulation area ratio (AAR) along a balance gradient curve would reduce uncertainty (Braithwaite and Raper, 2009; Pelto, 2011). However these methods are time and resource intensive and require *in situ* field visits. The ELA values used in our analysis will have an associated uncertainty of (+/- 20 meters), as this is the spatial resolution of the DEM used to determine elevation values. It has been suggested that all known ELA series show highly variability between successive years, corresponding to years with highly negative or positive mass balances (Braithwaite and Raper, 2009). The Lowell Glacier is no different, and ELA observations should be considered as qualitative estimations rather than precise quantitative measurements.

4. Results

Our findings indicate that the Lowell Glacier exhibits a negative overall mass balance trend from 1973 to 2018. This is consistent with an average annual temperature increase in the Alaska-Yukon region (Government of Yukon, 2018; Stafford et al., 2000). ELA on the Lowell Glacier demonstrates an increasing trend during the quiescent phases leading up to a surge event, and a decreasing trend during the active phase and the years following (Fig. 3). This is indicative of a negative relative mass balance during quiescent phases, which contradicts our hypothesis. As indicated in Figure 4, ELA increases as much as 280 meters (1975) during the quiescent phase following the 1968 surge event (A2). ELA decreased as much as 100 meters in active surge years (e.g. A4), which can be explained by ice thinning due surface

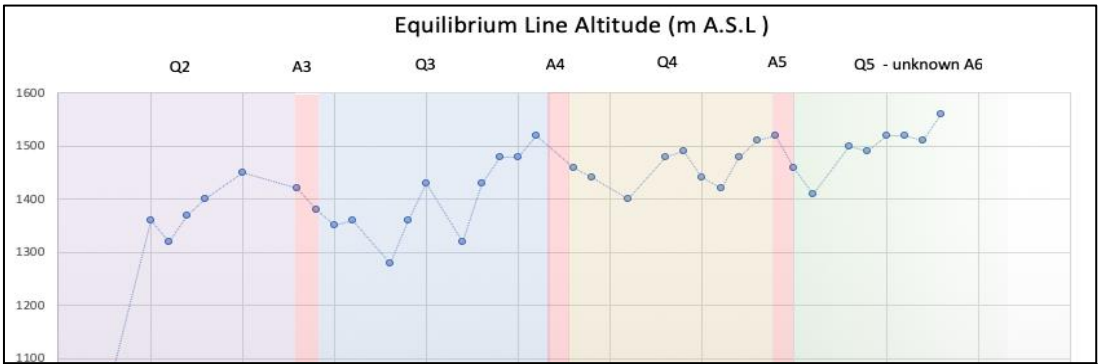

Fig. 3. ELA timeseries (1973-2018): ELA derived from snowline at the end of the balance year (late August – early September) using satellite imagery. Surge events derived from Bevington and Copland (2014); categorized into quiescent and active phases.

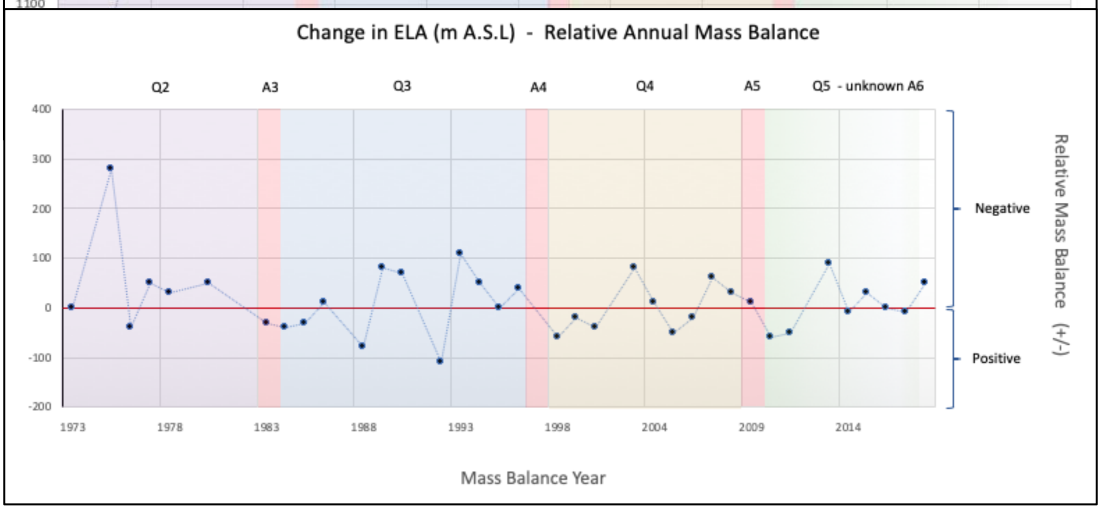

Fig. 4. Change in ELA (1973-2018): Change depicted as the difference in ELA between successive years. Reference line (ELA = 0 m a.s.l) is the first recorded ELA in our dataset (1973). Relative mass balances is divided into positive and negative categories depending on decreases and increases in ELA over one balance year respectively.

area increases, resulting in extensive ablation during the surge (Bevington and Copland, 2014; Sharp, 1988).

During active surge years (A3-A5), ELA on the Lowell Glacier decreases, then gradually starts to increase after 2-3 years following the surge event. There seems to be an observable lag period for which the glacier adjusts the ELA to account for the change in surface area and ice thickness. This indicates that the positive mass balance during these years is more or less a response to, rather than a driver of surge events. Figures 3 and 4 show that the surging process for the Lowell Glacier is not necessarily initiated by a mass balance threshold. If this hypothesis were true, it would be highly improbable to see ELA increasing during quiescent periods, since mass balance and ELA are closely related (Braithwaite and Raper, 2009; Mernild et al., 2013).

Since 1948, the average interval between successive surges on Lowell Glacier is 15.25 years and appears to be decreasing over time (Bevington and Copland, 2014) and ELA on the Lowell Glacier increased from 1080 to 1560 meters above sea level from 1973-2018. Our analysis suggests that the increasing surge frequency is most likely due to the negative mass balance trend as indicated by the ELA timeseries (fig. 3). However, figure 4 shows that the Lowell Glacier does not necessarily share the same mass balance – recurrence interval relationship as other Alaska-Yukon glaciers such (e.g. Variegated glacier), where a higher net annual mass balance leads to a shorter recurrence interval between surge events (Eisen et al., 2001). This is unclear in our analysis, as no obvious ELA trends are observed. A timeseries of cumulative mass balance is needed to establish this relationship.

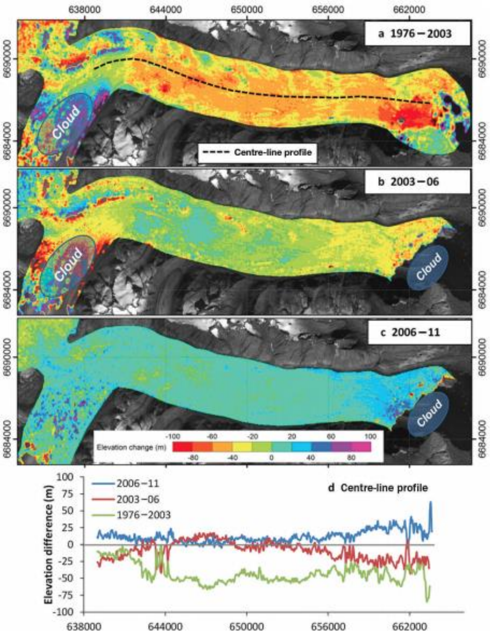

Fig. 5. Difference between DEMs of the of Lowell Glacier: ablation area: (a) 1976–2003 (Q2–Q4); (b) 2003–06 (Q4); (c) 2006–11 (A5); (d) centre-line profiles of DEM Difference. Elevation changes that could not be calculated due to cloud cover are identified by cloud symbol. (Bevington and Copland, 2014)

Figure 5 (taken from Bevington and Copland, (2014)), illustrates the dynamic elevation changes that are occurring in the ablation during active surge years, which may help to explain patterns of positive/negative mass balance in the surging process. Here we see a decrease of up to 2.2 m/yr across the main ablation area and 3.7 m/yr near the terminus of Lowell Glacier using a 1976-2003 DEM comparison.

5. Discussion and Conclusions

In this study, we expand on previous work on the Lowell Glacier to better understand this relationship between mass balance and cyclic surging events. Remotely sensed images have allowed us to track the Lowell Glacier ELA from 1973 – 2018, which indicates relative mass balance conditions. We have shown a positive (increasing) ELA trend since 1973, which is correlated with an average annual temperature increase in the region. This indicates a negative mass balance trend during this time, which is consistent with previous work showing a decrease in surface elevation of the main ablation area and near the terminus of Lowell Glacier (fig. 5), (Bevington and Copland, 2014), as well as a sustained and rapid thinning of 0.78 ± 0.34 m yr^{-1} water equivalent Yukon glaciers since the 1957 (Barrand and Sharp, 2010).

Furthermore, our analysis suggests that mass balance conditions are most likely driven by climate as opposed to the surging process, since our ELA time series does not exhibit a net positive mass balance during quiescent phases. This indicates that the surging process is not initiated by a mass balance threshold (e.g. Variegated Glacier), since the mass balance relationship demonstrates a lagged response to surging events (fig. 4). Eisen and others (2001) show that the surging process for Variegated Glacier is driven by net positive cumulative mass balance conditions, which does not coincide with our findings. The different mass balance-surging relationships among these two glaciers may be better explained by differences in thermal regime (bed characteristics), as well as subglacial meltwater drainage systems as specified in previous research in the Alaska-Yukon region (Fowler, 1987; Harrison and Post, 2003; Lingle and Fatland, 2003).

Although we do not have direct evidence observations of bed characteristics, it has been suggested that Lowell Glacier surges are initiated by a hydrological switch, where the subglacial drainage system changes from inefficient constricted to efficient channelized (Bevington and Copland, 2014). This implies that surges are most likely the result of build-up of mass in the accumulation area due to insufficient motion of the ablation area during quiescent periods, followed by the down-slope transport of mass which is initiated by subglacial drainage patterns (Kamb et al., 1985; Murray et al., 1998). These findings were derived from relative area, length, surface velocity changes, along with surface elevation changes (fig.5) during the Lowell Glacier's last five surges. Nevertheless, the mass balance - surging relationship is can most likely *indirect* according to our findings. Further research is needed to quantify cumulative mass balance in both the accumulation and ablation areas before and after surging events, however we infer from our results and that of previous works that the Lowell Glacier will not exhibit a mass balance threshold for surging initiation.

We would suggest that detailed studies on ice thickness in the accumulation area of Lowell Glacier would indicate how the surging initiation mechanism is related to mass build-up, rather than annual mass balance. DEM comparisons have been shown to be useful in this regard (Bevington and Copland, 2014), as well as snow depth measurements and calibration of AAR to a balance gradient curve (Hock et al., 2007; Pelto, 2011). Information regarding the build-up and downslope transfer of mass will be important in forecasting surges for not only the Lowell, but other alpine valley Glaciers in the Alaska-Yukon region.

References

Abe, T., Furuya, M., & Sakakibara, D. (2016). Brief Communication: Twelve-year cyclic surging episodes at Donjek Glacier in Yukon, Canada. *The Cryosphere*, *10*(4), 1427-1432.

American Geophysical Union (AGU), M. Pelto (2018). Major July Meltdown on Lowell Glacier , Yukon. Retrieved April 1, 2019, from https://blogs.agu.org/fromaglaciersperspective/2018/08/29/major-late-july-meltdown-on-lowell-glacier-yukon/

Barrand, N. E., & Sharp, M. J. (2010). Sustained rapid shrinkage of Yukon glaciers since the 1957–1958 International Geophysical Year. *Geophysical Research Letters*, *37*(7).

Bevington, A., & Copland, L. (2014). Characteristics of the last five surges of Lowell Glacier, Yukon, Canada, since 1948. *Journal of Glaciology*, *60*(219), 113-123.

Braithwaite, R. J., & Raper, S. C. B. (2009). Estimating equilibrium-line altitude (ELA) from glacier inventory data. Annals of Glaciology, 50(53), 127-132.

Clague JJ and Rampton VR (1982) Neoglacial Lake Alsek. Can. J. Earth Sci., 19(1), 94–117 (doi: 10.1139/e82-008)

Copland, L., Sylvestre, T., Bishop, M. P., Shroder, J. F., Seong, Y. B., Owen, L. A., ... & Kamp, U. (2011). Expanded and recently increased glacier surging in the Karakoram. *Arctic, Antarctic, and Alpine Research*, *43*(4), 503-516.

Dowdeswell, J. A., Hodgkins, R., Nuttall, A. M., Hagen, J. O., & Hamilton, G. S. (1995). Mass balance change as a control on the frequency and occurrence of glacier surges in Svalbard, Norwegian High Arctic. Geophysical Research Letters, 22(21), 2909-2912.

Eisen, O., Harrison, W. D., & Raymond, C. F. (2001). The surges of Variegated Glacier, Alaska, USA, and their connection to climate and mass balance. *Journal of Glaciology*, *47*(158), 351-358.

Flowers, G. E., Copland, L., & Schoof, C. G. (2014). Contemporary glacier processes and global change: recent observations from Kaskawulsh Glacier and the Donjek Range, St. Elias Mountains. Arctic, 22-34.

Flowers GE, Roux N, Pimentel S and Schoof CG (2011) Present dynamics and future prognosis of a slowly surging glacier. Cryosphere, 5(1), 299–313

Fowler, A. C. (1987). A theory of glacier surges. *Journal of Geophysical Research: Solid Earth*, *92*(B9), 9111-9120.

GKC and Holdsworth, G. (2002). Glaciers of the St Elias Mountains. In Williams RS Jr and Ferrigno JG eds. Satellite image atlas of glaciers of the world: glaciers of North America–glaciers of Canada. *(USGS Professional Paper 1386-J) US Geological Survey,* J301–J328

Government of Yukon, (2018). State of Environment Report. Retrieved April 1, 2019, from http://www.env.gov.yk.ca/publications-maps/report-air-yukon-temperature.php

Hall DK, Chang ATC, Foster JL, Benson CS and Kovalick WM (1989) Comparison of *in situ* and Landsat derived reflectance of Alaskan glaciers. Remote Sens. Environ., 28, 23–31 (doi:10.1016/0034-4257(89)90102-8)

Harrison, W. D., & Post, A. S. (2003). How much do we really know about glacier surging? *Annals of glaciology*, *36*, 1-6.

Hock R, Kootstraa D-S and Reijmer C (2007) Deriving glacier mass balance from accumulation area ratio on Storglaciären, Sweden. *IAHS Publ.* 318 (Symposium at Foz do Iguaçu 2005 – *Glacier* Mass Balance Changes and Meltwater Discharge), 163–170

Kamb B and 7 others (1985) Glacier surge mechanism: 1982–1983 surge of Variegated Glacier, Alaska. Science, 227(4686), 469–479

Lingle, C. S., & Fatland, D. R. (2003). Does englacial water storage drive temperate glacier surges?. Annals of Glaciology, 36, 14-20.

Meier, M. F., & Post, A. (1969). What are glacier surges?. *Canadian Journal of Earth Sciences*, *6*(4), 807-817.

Mernild, S. H., Pelto, M., Malmros, J. K., Yde, J. C., Knudsen, N. T., & Hanna, E. (2013). Identification of snow ablation rate, ELA, AAR and net mass balance using transient snowline variations on two Arctic glaciers. *J. Glaciol*, *59*(216), 649-659.

Murray T, Dowdeswell JA, Drewry DJ and Frearson I (1998) Geometric evolution and ice dynamics during a surge of Bakaninbreen, Svalbard. J. Glaciol., 44(147), 263–272

Østrem G (1975) ERTS data in glaciology – an effort to monitor glacier mass balance from satellite imagery. *J. Glaciol.*, 15(73), 403–415

Pelto, M. (2011). Utility of late summer transient snowline migration rate on Taku Glacier, Alaska. *The Cryosphere, 5*(4), 1127-1133.

Sharp, M. (1988). Surging glaciers: behaviour and mechanisms. *Progress in Physical Geography*, *12*(3), 349-370.

Stafford, J. M., Wendler, G., & Curtis, J. (2000). Temperature and precipitation of Alaska: 50 year trend analysis. *Theoretical and Applied Climatology*, *67*(1-2), 33-44.